Vol. XV Nº 1 Junio (2007)
Matemáticas: 51–66

Matemáticas:
Enseñanza Universitaria

Pulsatile flow between two coaxial porous cylinders with slip on inner cylinder

Elsadig A. Hamza Satish C. Rajvanshi Nirmal C. Sacheti

Received Feb. 8, 2006 Accepted Mar. 22, 2007

Abstract

A fully developed, axisymmetric, pulsatile motion of an incompressible Newtonian fluid, under the action of an oscillatory pressure gradient, has been considered in this work. The flow is assumed to take place in the annular space between two coaxial circular cylinders, the outer one a porous cylinder of uniform permeability and the inner one a naturally permeable tube. There arises a coupled flow, which has been analysed by solving the Navier-Stokes equations in the free fluid region and the Darcy's equation in the porous region, together with the Beavers-Joseph slip condition at the free fluid-porous medium interface. Using an appropriate set of similarity variables, the governing partial differential equations have been transformed to a system of nonlinear ordinary differential equations. The solution of the resulting system, together with appropriate boundary conditions, has been obtained, for a special case, by a perturbation approach. It has been assumed that the frequency of pulsation and the suction parameter are small ($<< 1$). The variation of velocity profiles, pressure drop and skin friction has been illustrated in a number of cases of interest. The analytical results have been compared with numerical solution for small values of suction parameter.

Keywords: Pulsatile flow, similarity analysis, porous annulus, Darcy's law, Navier-Stokes equations

MSC(2000): 76M99, 76S05

1 Introduction

The mathematical analysis of viscous laminar flow through channels with porous walls has attracted a lot of attention due to their industrial applications and theoretical interest. Terrill [1] carried out a detailed study of the laminar flow through a porous annulus by assuming the swirl to be zero, and presented a series solution for small suction or injection. The work also included the asymptotic behaviour for large blowing or suction. In a subsequent work, Terrill [2] obtained general solution for the fully developed flow in a permeable annulus. Huang [3] corrected the first order solution [1] for small suction or injection. Verma and Gaur [4] investigated the flow in a porous annulus with surface mass transfer in radial as well as circumferential directions.

Skalak and Wang [5], Verma and Gaur [6] considered axial pulsatile flows between two porous cylinders. Singh and Rajvanshi [7],[8] conducted a detailed investigation on the viscous flow in a porous annulus under periodic pressure gradient. They employed regular perturbation techniques for small suction or injection while singular perturbation method was used to study the problem involving large suction at both the cylinders or for large values

of the frequency of pulsation. There is a good agreement between analytical and numerical results in their work.

The investigations of flow through porous media are important in numerous scientific and engineering applications, e.g. [9]. In particular, following the introduction of the Beavers-Joseph [10] slip condition at a naturally permeable boundary, a large number of viscous incompressible flows through porous channels, cylinders or between porous disks have been extended to the case when one or both boundaries are made of naturally permeable material [11],[14]. The present work is related to the pulsatile flow of a viscous incompressible flow in the annular space of a porous cylinder within which a naturally permeable tube is placed coaxially. It is assumed that the porous material is of small permeability and fully saturated with a viscous incompressible fluid. Using similarity transformation approach [7], we have been able to reduce the governing partial differential equations to a set of coupled nonlinear ODEs. The latter set of equations has been solved assuming the suction parameter and the frequency of the pulsation to be small and using BJ condition [10] at the surface of the inner permeable tube. The effect of various flow parameters has been discussed in relation to velocity profiles and pressure drop. The skin-friction at the surface of inner cylinder has also been discussed. For small values of suction Reynolds number the numerical computation has been done. These results have been compared with analytical results.

2 Governing equations and boundary conditions

A fully developed incompressible laminar flow in the region bounded by two long coaxial cylinders of radii a and b $(a < b)$ respectively is considered. The outer cylinder is porous and the inner cylindrical tube is made of a permeable material, with small permeability, and fully saturated. It is assumed that the flow is axisymmetric without any swirl velocity. A periodic pressure gradient is imposed across the annulus. In the cylindrical polar coordinate system (r, θ, z), the z-axis is taken along the common axis of the cylinders. Let u and w be the velocity components of the fluid in the positive directions of r and z respectively. The governing Navier-Stokes equations in the annular free fluid region $(a < r < b)$ are

$$\frac{\partial u}{\partial t} + u\frac{\partial u}{\partial r} + w\frac{\partial u}{\partial z} = -\frac{1}{\rho}\frac{\partial p}{\partial r} + \nu\left(\frac{\partial^2 u}{\partial r^2} + \frac{1}{r}\frac{\partial u}{\partial r} + \frac{\partial^2 u}{\partial z^2} - \frac{u}{r^2}\right) \tag{1}$$

$$\frac{\partial w}{\partial t} + u\frac{\partial w}{\partial r} + w\frac{\partial w}{\partial z} = -\frac{1}{\rho}\frac{\partial p}{\partial z} + \nu\left(\frac{\partial^2 w}{\partial r^2} + \frac{1}{r}\frac{\partial w}{\partial r} + \frac{\partial^2 w}{\partial z^2}\right) \tag{2}$$

The equation of continuity is

$$\frac{\partial u}{\partial r} + \frac{u}{r} + \frac{\partial w}{\partial z} = 0 \tag{3}$$

In the above equations, t is the time, p is the pressure, ρ is the fluid density and ν is the kinematic viscosity. The flow in the permeable tube follows Darcy's law. It is further assumed that the flow is entirely due to axial pressure gradient, so there is no radial flow. The governing equations with U and W as velocity components are

$$U = 0, \quad W = -\frac{k}{\mu}\frac{\partial P}{\partial z}, \tag{4}$$

k being the permeability of the porous medium and μ is the coefficient of viscosity. The boundary conditions on the outer cylinder are:

$$u = V, \ w = 0 \text{ at } r = b, \tag{5}$$

V being the suction velocity at the surface of the outer cylinder. The slip condition on the surface of the inner cylinder ($r = a$) is prescribed by the modified BJ condition, applicable at a curved surface (see, for instance [15],[16].

$$\frac{\partial u}{\partial z} + \frac{\partial w}{\partial r} = \gamma\,(w - W)\,, \tag{6}$$

where $\gamma = \dfrac{\alpha^*}{\sqrt{k}}$, α^* being a constant depending upon the porous medium. In addition, the continuity of normal velocity on the interface of the inner permeable material and the free fluid region is assumed.

Since the radial velocity is constant at the bounding wall, it is a function of the radial coordinate, r, only. It can thus be written as

$$u = \frac{1}{r}F\,(r)\,, \tag{7}$$

$F\,(r)$ being an arbitrary function to be determined. From (7) and the equation of continuity (3), it is easily found that

$$w = -\frac{z}{r}F'\,(r) + \phi\,(r,t)\,, \tag{8}$$

where $\phi(r,t)$ is an arbitrary function of r and t, while prime denotes ordinary derivative with respect to the variable r.

Equations (1), (7) and (8) yield:

$$-\frac{p}{\rho} = \frac{1}{2}\left(\frac{F}{r}\right)^2 - \nu\left(\frac{F'}{r}\right) + p_1\,(z,t) \tag{9}$$

As the flow is pulsatile in nature, $p_1(z,t)$ and $\phi(r,t)$ can be taken in the form [7]:

$$p_1\,(z,t) = L_1 z^2 - L_2 z + L_3 + \mathrm{Re}\left[(L_4 z + L_5)\exp\,(i\omega t)\right], \tag{10}$$

$$\phi(r,t) = G(r) + \mathrm{Re}\left[H(r)\exp(i\omega t)\right], \tag{11}$$

where Re stands for "real part of" and ω is the frequency of pulsation.

From equations (7) to (11) one may notice that the velocity components, u and w, and the pressure, p, are now expressed in terms of arbitrary functions, $F(r)$, $G(r)$ and $H(r)$, which need to be determined. On using these equations, (7) to (11), in the equation (2), we can easily obtain a set of ordinary, nonlinear differential equations connecting F, G and H. The corresponding boundary conditions are obtained by using these equations in conjunction with equations (4), (5) and (6) together with continuity of pressure at the interface of free fluid region and permeable medium. The continuity requirement of the radial velocity at $r = a$ has also been maintained. The details of the derivation are recorded in Appendix. However, the non-dimensional form of the equations connecting the arbitrary functions, along with boundary conditions, can be obtained by introducing the following non-dimensional variables:

$$r = b\sqrt{\eta}, F(r) = bVf(\eta), G(r) = Vg(\eta), H(r) = \left(\frac{L_4 b^2}{4\nu}\right) h(\eta) \tag{12}$$

After a bit of algebra, it can be shown that the ODEs satisfied by newly introduced functions, f, g, and h, are given by

$$\eta f''' + f'' + \frac{1}{2}R\left(f'^2 - ff''\right) = \beta \tag{13}$$

$$\eta g'' + g' + \frac{1}{2}R\left(gf' - g'f\right) = d \tag{14}$$

$$\eta h'' + h' - i\alpha^2 h + \frac{1}{2}R\left(hf' - h'f\right) = -1 \tag{15}$$

where a set of non-dimensional parameters is defined as

$$\beta = -\frac{Rb^2 L_1}{4V^2}, \quad d = \frac{L_2 b^2}{4\nu V}, \quad \alpha^2 = \frac{\omega b^2}{4\nu}, \quad R = \frac{bV}{\nu}, \tag{16}$$

were R stands for the Reynolds number.

In the equations (13) through (15), primes now denote derivatives of various orders with respect to η while the parameter α now characterizes the frequency of pulsation. It may be remarked that the equations (13) and (14) depict the steady flow while the equation (15) correspond to the unsteady component of the flow.

In terms of similarity functions, the boundary conditions can be shown to be given by

$$f(1) = 1, f'(1) = 0, g(1) = 0, h(1) = 0, \tag{17}$$

$$f''(\eta_0) - \frac{1}{\lambda}f'(\eta_0) + \frac{\beta}{\lambda}C^* = 0, \quad g'(\eta_0) - \frac{1}{\lambda}g(\eta_0) - \frac{d}{\lambda}C^* = 0, \tag{18}$$

$$h'(\eta_0) - \frac{1}{\lambda} h(\eta_0) + \frac{1}{\lambda} C^* = 0, \quad f(\eta_0) = 0 \tag{19}$$

where, another set of non-dimensional parameters, is

$$\lambda = \frac{2a}{\gamma b^2}, C^* = \frac{4k}{b^2}, \eta_0 = \frac{a^2}{b^2}. \tag{20}$$

3 Solution of governing ODEs

We now proceed to solve the set of coupled nonlinear ODEs (13) to (15), subject to the boundary conditions (17) to (18), analytically. To facilitate this, we first of all resort to the approach of Skalak and Wang [5] and thus assume a particular solution of equation (14) as

$$g(\eta) = -\frac{L_2 f'(\eta)}{b L_1} \tag{21}$$

In view of (21), the ODEs (13) and (15) only need to be solved. Introducing$\in = R/2$ we can rewrite equations (13) and (15) as

$$\eta f''' + f'' + \in \left(f'^2 - f f''\right) = \beta \tag{22}$$

$$\eta h'' + h' - i\alpha^2 h + \in \left(h f' - h' f\right) = -1 \tag{23}$$

Assuming $\in$ to be small and positive, we next seek solutions of (22) and (23) as regular perturbation solutions, in powers of $\in$, by assuming

$$f(\eta) = f_0(\eta) + \in f_1(\eta) + O\left(\in^2\right) \tag{24}$$

$$h(\eta) = h_0(\eta) + \in h_1(\eta) + O\left(\in^2\right) \tag{25}$$

$$\beta = \beta_0 + \in \beta_1 + O\left(\in^2\right) \tag{26}$$

Note that we are effectively finding solutions for small suction at the boundary surface of the outer cylinder. We next set out to obtain perturbation equations for $f(\eta)$ and $h(\eta)$.

3.1 Perturbed equations: steady components

The zeroth and first order perturbed equations for $f(\eta)$, together with boundary conditions, can be easily obtained from equations (22), (24), (26) and relevant equations in (17) to (19). After some algebra, the various order equations and associated boundary conditions can be shown to be given by:

$$\begin{aligned} \eta f_0''' + f_0'' &= \beta_0, \\ \eta f_1''' + f_1'' &= \beta_1 - f_0'^2 + f_0 f_0'' \end{aligned} \tag{27}$$

$$
\begin{aligned}
f_0(1) = 1, f_0'(1) = 0, f_1(1) = 0, f_1'(1) = 0,\\
f_0(\eta_0) = 0, f_0''(\eta_0) - \frac{1}{\lambda} f_0'(\eta_0) + \frac{1}{\lambda}\beta_0 C^* = 0,\\
f_1(\eta_0) = 0, f_1''(\eta_0) - \frac{1}{\lambda} f_1'(\eta_0) + \frac{1}{\lambda}\beta_1 C^* = 0
\end{aligned} \tag{28}
$$

The solutions of linear ODEs (27), subject to the boundary conditions above, have been obtained as

$$
f_0(\eta) = A_1 + A_2\eta + A_3\eta\ln\eta + \frac{1}{2}\beta_0\eta^2 \tag{29}
$$

$$
\begin{aligned}
f_1(\eta) = {} & B_0 + B_1\eta + B_2\eta\ln\eta + \left(\frac{1}{2}\beta_1 + B_3\right)\eta^2 + B_4\eta(\ln\eta)^2 + B_5\eta^3\\
& + B_6\eta^4 + B_7\eta^2\ln\eta + B_8\eta^3\ln\eta + B_9\eta^2(\ln\eta)^2
\end{aligned} \tag{30}
$$

where $N_0 = \ln\eta_0$ and

$$
\begin{aligned}
A_1Q_0 &= -\eta_0^2 + \eta_0^3 - \frac{1}{2}\eta_0^3 N_0 + \lambda\left(\eta_0 - \frac{3}{2}\eta_0^2 + \eta_0^2 N_0\right) + C^*\eta_0^2(-1 + N_0)\\
A_2Q_0 &= \eta_0 - \eta_0^2 + \eta_0 N_0 + \lambda(-1 + \eta_0) + C^*\eta_0\\
A_3Q_0 &= -\eta_0 + \eta_0^2 - \lambda\eta_0 - C^*\eta_0\\
\beta_0Q_0 &= \lambda - \eta_0 N_0\\
Q_0 &= \eta_0 - 2\eta_0^2 + \eta_0^3 + \frac{1}{2}\eta_0 N_0 - \frac{1}{2}\eta_0^3 N_0\\
&\quad + \lambda\left(-\frac{1}{2} + 2\eta_0 - \frac{3}{2}\eta_0^2 + \eta_0^2 N_0\right) + C^*\left(\eta_0 - \eta_0^2 + \eta_0^2 N_0\right)\\
B_0Q_1 &= \frac{1}{2}C_1\left(\eta_0 - \eta_0^2 + \eta_0 N_0\right) + C_2\left(-1 + \eta_0 - \frac{1}{2}N_0 - \lambda + \frac{\lambda}{2\eta_0}\right)\\
&\quad + C_3\left[\left(\eta_0 - \eta_0^2 + \frac{1}{2}\eta_0^2 N_0\right) + \lambda\left(-1 + \frac{3}{2}\eta_0 - \eta_0 N_0\right)\right]\\
&\quad + C_4\left[\frac{1}{2}\eta_0(-1 + \eta_0 - \eta_0 N_0) + \frac{1}{2}\lambda(1 - \eta_0 + 2\eta_0 N_0)\right]\\
&\quad + C^*\left[C_3\eta_0(1 - N_0) + C_4\eta_0 N_0 - C_2\right]\\
B_1Q_1 &= \frac{1}{2}C_1\left(-1 + \eta_0^2 - 2\eta_0 N_0\right) + C_2\left(1 - \eta_0 + N_0 + \lambda - \frac{\lambda}{\eta_0}\right)\\
&\quad + C_3\left(-1 + \eta_0 - N_0 - \lambda + \frac{\lambda}{\eta_0}\right)\\
&\quad + C_4\left[\frac{1}{2}\left(1 - \eta_0^2 + N_0 + \eta_0^2 N_0\right) + \frac{1}{2}\lambda\left(\eta_0 - 2\eta_0 N_0 - \frac{1}{\eta_0}\right)\right]
\end{aligned}
$$

$$
\begin{aligned}
&+ C^* \left(C_2 - C_3 - C_4\eta_0 N_0\right)\\
B_2Q_1 &= \frac{1}{2}C_1\left(-1+2\eta_0-\eta_0^2\right) + C_2(-1+\eta_0-\lambda) + C_3\left(1-\eta_0+\lambda\right)\\
&+ \frac{1}{2}C_4\left(-1+2\eta_0-\eta_0^2-2\lambda+2\lambda\eta_0\right) + C^*\left[-C_2+C_3+C_4\left(-1+\eta_0\right)\right]\\
\beta_1Q_1 &= C_1\left(1-\eta_0+\eta_0N_0\right) + C_2(-N_0+\frac{\lambda}{\eta_0}) + C_3\left(N_0-\frac{\lambda}{\eta_0}\right)\\
&+ C_4\left(-1+\eta_0-N_0-\lambda+\frac{\lambda}{\eta_0}\right)\\
Q_1 &= -1+2\eta_0-\eta_0^2-\frac{1}{2}N_0+\frac{1}{2}\eta_0^2N_0+\lambda\left(-2+\frac{3}{2}\eta_0-\eta_0N_0+\frac{1}{2\eta_0}\right)\\
&+ C^*\left(-1+\eta_0-\eta_0N_0\right)\\
B_3 &= \frac{1}{2}A_1\beta_0 - \frac{1}{2}A_2^2 - \frac{7}{2}A_3^2 + 2A_2A_3\\
B_4 &= \frac{1}{2}A_1A_3, \quad B_5 = -\frac{1}{72}\beta_0\left(A_3+6A_2\right), \quad B_6 = -\frac{1}{72}\beta_0^2\\
B_7 &= 2A_3^2 - A_2A_3, \quad B_8 = -\frac{1}{12}A_3\beta_0, \quad B_9 = -\frac{1}{2}A_3^2\\
C_1 &= 2B_3\left(-\eta_0+\lambda\right) + B_4\left(-2N_0-N_0^2+\frac{2\lambda}{\eta_0}+\frac{2\lambda}{\eta_0}N_0\right)\\
&+ B_5\left(-3\eta_0^2+6\lambda\eta_0\right) + B_6\left(-4\eta_0^3+12\lambda\eta_0^2\right)\\
&+ B_7\left(-\eta_0-2\eta_0N_0+3\lambda+2\lambda\eta_0\right)\\
&+ B_8\left(-\eta_0^2-3\eta_0^2N_0+5\lambda\eta_0+6\lambda\eta_0N_0\right)\\
&+ B_9\left(-2\eta_0N_0-2\eta_0N_0^2+2\lambda+6\lambda N_0+2\lambda N_0^2\right)\\
C_2 &= -B_3\eta_0^2 - B_4\eta_0N_0^2 - B_5\eta_0^3 - B_6\eta_0^4\\
&- B_7\eta_0^2N_0 - B_8\eta_0^3N_0 - B_9\eta_0^2N_0^2\\
C_3 &= -B_3 - B_5 - B_6, C_4 = -2B_3 - 3B_5 - 4B_6 - B_7 - B_8
\end{aligned}
$$

3.2 Perturbed equations: unsteady component

Having obtained analytical solution for $f(\eta)$, and hence $g(\eta)$, we now proceed to solve the coupled second order nonlinear ODE(23) for $h(\eta)$. The equations (23) and (25) can be shown to yield the following set of equations for the function $h(\eta)$:

$$\eta h_0'' + h_0' - i\alpha^2 h_0 = -1, \quad \eta h_1'' + h_1' - i\alpha^2 h_1 = f_0h_0' - f_0'h_0, \tag{31}$$

while the associated set of boundary conditions are:

$$
\begin{aligned}
h_0(1) = 0, \quad h_0'\left(\eta_0\right) - \frac{1}{\lambda}h_0\left(\eta_0\right) + \frac{1}{\lambda}C^* = 0,\\
h_1(1) = 0, h_1'\left(\eta_0\right) - \frac{1}{\lambda}h_1\left(\eta_0\right) = 0
\end{aligned} \tag{32}
$$

The solution of the set of equations in (31) is sought in the form:

$$h_0(\eta) = s_0(\eta) + \alpha^2 s_1(\eta) + \alpha^4 s_2(\eta) + O\left(\alpha^6\right)$$
$$h_1(\eta) = q_0(\eta) + \alpha^2 q_1(\eta) + O\left(\alpha^4\right) \tag{33}$$

It is worth mentioning that perturbation solutions (33) above correspond to the assumption that the frequency of pulsation, ω, is small. For large value of ω (i.e., $\alpha^2 >> 1$), the problem leads to a singular perturbation problem. This type of flow will be discussed in a separate study.

By substituting (33) into (31) and (32), and equating coefficients of like powers of α^2, we can obtain a system of ordinary differential equations together with a set of modified boundary conditions. The solution of such a system of boundary-value problems has been obtained, by a straight-forward integration, as

$$h_0(\eta) = 1 - \eta + E_1 \ln\eta + i\alpha^2[-\overline{C_2} + \overline{C_3}\ln\eta + m_1(\eta)] + \alpha^4[E_6 + E_5\ln\eta + g_2(\eta)], \tag{34}$$

where

$$m_1(\eta) = \eta - \frac{1}{4}\eta^2 + E_1(\eta\ln\eta - 2\eta) \quad \overline{C_2} = \frac{3}{4} - 2E_1 \tag{35}$$

$$g_2(\eta) = \overline{C_2}\eta - \overline{C_3}(\eta\ln\eta - 2\eta) - \frac{1}{4}\eta^2 + \frac{1}{36}\eta^3 + \frac{1}{4}E_1\eta^2(3 - \ln\eta) \tag{36}$$

$$E_1(\lambda - \eta_0 N_0) = \eta_0(-\eta_0 + \lambda + 1 - C^*) \tag{37}$$

$$\overline{C_3}(\lambda - \eta_0 N_0) = \eta_0\left[m_1(\eta_0) - \lambda m_1'(\eta_0) - \frac{3}{4} + 2E_1\right] \tag{38}$$

$$E_5(\lambda - \eta_0 N_0) = \eta_0\left[g_2(\eta_0) - g_2(1) - \lambda g_2'(\eta_0)\right] \quad E_6 = -g_2(1), \tag{39}$$

while the expression for the perturbed quantity, $h_1(\eta)$, is given by

$$\begin{aligned} h_1(\eta) = {} & D_1 + D_2\ln\eta + \eta(-A_1 - A_2 + A_3 + 3A_2E_1 - 6A_3E_1) \\ & + \frac{1}{8}\eta^2(3\beta_0E_1 - 2\beta_0 + 2A_3) + \frac{1}{18}\eta^3\beta_0 \\ & + \frac{1}{2}A_1E_1(\ln\eta)^2 + \eta\ln\eta(-A_3 - A_2E_1 + 4A_3E_1) \\ & - A_3E_1\eta(\ln\eta)^2 - \frac{1}{4}\beta_0E_1\eta^2\ln\eta + i\alpha^2[\overline{D_3} + \overline{D_4}\ln\eta \\ & + \eta\left(D_1 + A_1 + 3A_2\overline{C_3} + A_2\overline{C_2} - A_3\overline{C_2} - 2D_2 - 6A_3\overline{C_3}\right) \\ & + \frac{1}{8}\eta^2\left(-3A_1 - 2A_2 + 10A_2E_1 - 19A_3E_1 + 3\beta_0\overline{C_3} + 2\beta_0\overline{C_2} + 2A_3\right) \\ & + \frac{1}{216}\eta^3(57\beta_0E_1 - 18\beta_0 + 16A_3 - 6A_2) \\ & + \frac{1}{288}\eta^4\beta_0 + \eta\ln\eta\left(D_2 - A_1E_1 - A_2\overline{C_3} + A_3\overline{C_2} + 4A_3\overline{C_3}\right) \end{aligned}$$

$$
\begin{aligned}
&- \frac{1}{4}\eta^2 \ln\eta \left(A_3 - 6A_3E_1 + A_2E_1 + \beta_0\overline{C_3}\right) \\
&- \frac{1}{36}\eta^3 \ln\eta \left(3\beta_0E_1 + A_3\right) + \frac{1}{2}A_1\overline{C_3}\left(\ln\eta\right)^2 \\
&+ \frac{1}{2}\eta\left(\ln\eta\right)^2\left(A_1E_1 - 2A_3\overline{C_3}\right) - \frac{1}{4}A_3E_1\eta^2\left(\ln\eta\right)^2], \qquad (40)
\end{aligned}
$$

where $D_1 = A_1 + A_2 - \frac{5}{4}A_3 - 3A_2E_1 + 6A_3E_1 - \frac{3}{8}\beta_0E_1 + \frac{7}{36}\beta_0$ and

$$
\begin{aligned}
D_2\left(\lambda - \eta_0N_0\right) &= \lambda\eta_0\left(A_1 + A_2 - 2A_2E_1 + 2A_3E_1\right) \\
&- \frac{1}{2}\lambda\eta_0^2\left(\beta_0E_1 - \beta_0 + A_3\right) - \frac{1}{6}\lambda\beta_0\eta_0^3 - \lambda A_1E_1N_0 \\
&+ \lambda\eta_0N_0\left(A_3 + A_2E_1 - 2A_3E_1\right) + \lambda A_3E_1\eta_0N_0^2 \\
&+ \frac{1}{2}\lambda\beta_0E_1\eta_0^2N_0 + \frac{1}{36}\eta_0(36A_1 + 36A_2 - 45A_3 \\
&- 108A_2E_1 + 216A_3E_1 - \frac{27}{2}\beta_0E_1 + 7\beta_0) \\
&- \eta_0^2\left(A_1 + A_2 - A_3 - 3A_2E_1 + 6A_3E_1\right) \\
&+ \frac{1}{8}\eta_0^3(3\beta_0E_1 - 2\beta_0 + 2A_3) \\
&+ \frac{1}{18}\beta_0\eta_0^4 + \frac{1}{2}A_1E_1\eta_0N_0^2 - \eta_0^2N_0(A_3 + A_2E_1 - 4A_3E_1) \\
&- A_3E_1\eta_0^2N_0^2 - \frac{1}{4}\beta_0E_1\eta_0^3N_0
\end{aligned}
$$

$$
\begin{aligned}
\overline{D_3} &= -D_1 - \frac{5}{8}A_1 - 3A_2\overline{C_3} - A_2\overline{C_2} + A_3\overline{C_2} + 2D_2 + 6A_3\overline{C_3} + \frac{5}{18}A_2 \\
&- \frac{5}{4}A_2E_1 + \frac{19}{8}A_3E_1 - \frac{3}{8}\beta_0\overline{C_3} - \frac{1}{4}\beta_0\overline{C_2} - \frac{35}{108}A_3 - \frac{19}{72}\beta_0E_1 + \frac{23}{288}\beta_0
\end{aligned}
$$

$$
\begin{aligned}
\overline{D_4}\left(\frac{\lambda}{\eta_0} - N_0\right) &= -D_1 - \frac{5}{8}A_1 - 3A_2\overline{C_3} - A_2\overline{C_2} + A_3\overline{C_2} + 2D_2 \\
&+ 6A_3\overline{C_3} + \frac{5}{18}A_2 - \frac{5}{4}A_2E_1 + \frac{19}{18}A_3E_1 - \frac{3}{8}\beta_0\overline{C_3} \\
&- \frac{1}{4}\beta_0\overline{C_2} - \frac{35}{108}A_3 - \frac{19}{72}\beta_0E_1 + \frac{23}{288}\beta_0 \\
&+ \eta_0(D_1 + A_1 + 3A_2\overline{C_3} + A_2\overline{C_2} - A_3\overline{C_2} - 2D_2 - 6A_3\overline{C_3}) \\
&+ \frac{1}{72}\eta_0^3(19\beta_0E_1 - 6\beta_0 + \frac{16}{3}A_3 - 2A_2) \\
&+ \frac{1}{288}\beta_0\eta_0^4 + \eta_0N_0(D_2 - A_1E_1 - A_2\overline{C_3} + A_3\overline{C_2} + 4A_3\overline{C_3}) \\
&- \frac{1}{4}\eta_0^2N_0\left(A_3 - 6A_3E_1 + A_2E_1 + \beta_0\overline{C_3}\right) \\
&+ \frac{1}{8}\eta_0^2\left(-3A_1 - 2A_2 + 10A_2E_1 - 19A_3E_1 + 3\beta_0\overline{C_3} + 2\beta_0\overline{C_2} + 2A_3\right)
\end{aligned}
$$

$$
\begin{aligned}
&-\frac{1}{36}\eta_0^3 N_0\left(3\beta_0 E_1+A_3\right)+\frac{1}{2}A_1\overline{C_3}N_0^2+\frac{1}{2}\eta_0 N_0^2\left(A_1E_1-2A_3\overline{C_3}\right)\\
&-\frac{1}{4}A_3E_1\eta_0^2N_0^2+\lambda\left(-D_1-A_1-2A_2\overline{C_3}-A_2\overline{C_2}+D_2+2A_3\overline{C_3}+A_1E_1\right)\\
&+\frac{1}{4}\lambda\eta_0\left(3A_1+2A_2-9A_2E_1+13A_3E_1-2\beta_0\overline{C_3}-2\beta_0\overline{C_2}-A_3\right)\\
&+\frac{1}{72}\lambda\eta_0^2\left(-51\beta_0E_1+18\beta_0-14A_3+6A_2\right)-\frac{1}{72}\beta_0\eta_0^3\\
&-\frac{1}{\eta_0}\lambda A_1\overline{C_3}N_0+N_0\left(-D_2+A_2\overline{C_3}-A_3\overline{C_2}-2A_3\overline{C_3}\right)\\
&+\frac{1}{2}\lambda\eta_0N_0\left(A_3-5A_3E_1+A_2E_1+\beta_0\overline{C_3}\right)+\frac{1}{12}\lambda\eta_0^2N_0\left(3\beta_0E_1+A_3\right)\\
&-\frac{1}{2}\lambda N_0^2\left(A_1E_1-2A_3\overline{C_3}\right)+\frac{1}{2}\lambda A_3E_1\eta_0N_0^2
\end{aligned}
$$

4 Discussion

For numerical work the value of (a/b) is fixed at 0.5, so that $\eta_0 = 0.25$.

4.1 Velocity profiles

The variations of radial and axial velocity profiles have been shown in Figs. 1 through 5. 1 shows the radial velocity profiles for $R = 0.05$ and $\lambda = 0.1$. The effect of the parameter C^* has been depicted on these profiles. With increase in the value of this parameter, the magnitude of radial velocity is decreased in the free fluid region. The 2 illustrates the effect of the suction Reynolds number, R, on radial velocity profiles for a fixed $C^*\,(= 0.05)$ and $\lambda\,(= 0.1)$. With an increase in R, the magnitude of radial velocity can be seen to enhance, although the quantitative difference is now less marked (cf. profiles in Figs. 1 and 2). The 3 shows the effect of C^* on axial velocity profiles. It is interesting to note that the slip velocity on the surface of the inner permeable cylinder is more pronounced for small C^*. An increase in C^* apparently decreases the slip on the inner surface. Furthermore, the axial velocity assumes a maximum in a region which is nearer to this inner cylinder. The 4 exhibits the effect of the suction Reynolds number (R) on the axial velocity profiles. An increase in R has a tendency to enhance the velocity slip on the permeable (inner) cylinder, a phenomenon similar to that observed in the previous Figure but less pronounced. In the 5, we have shown unsteady (fluctuating) component of axial velocity for $R = 0.05, \alpha^2 = 0.01, C^* = 0.05$ and $\lambda = 0.1$ at different times. It is noted that axial velocity profiles have critical points closer to the inner boundary because of the forward momentum imparted to the flow by the permeable surface. The critical points occur at $\eta = 0.450$ for $\omega t = 0, 3\pi/4$ and π. There is a slight variation in case of $\omega t = \pi/4$; it has been observed to occur at $\eta = 0.455$. This fluctuating component of velocity can be seen to reverse its direction for values of ωt

between $\pi/2$ and π, thus likely to have considerable effect on the resulting axial velocity.

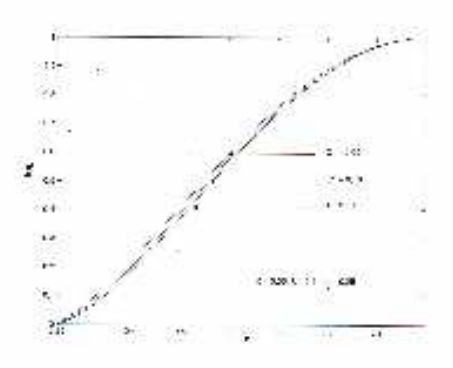

Figure 1: Variation of Radial Velocity (for fixed R)

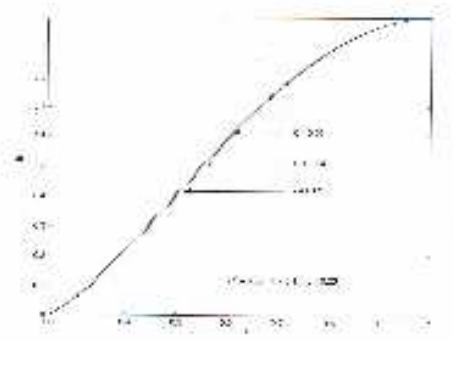

Figure 2: Variation of Radial Velocity (for fixed C^*)

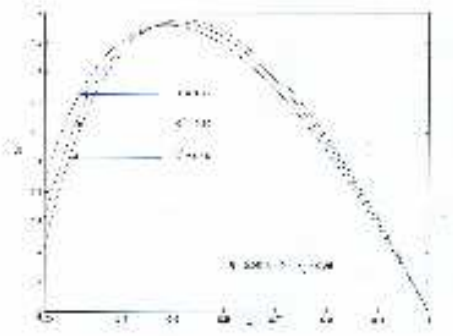

Figure 3: Variation of Axial Velocity (for fixed R)

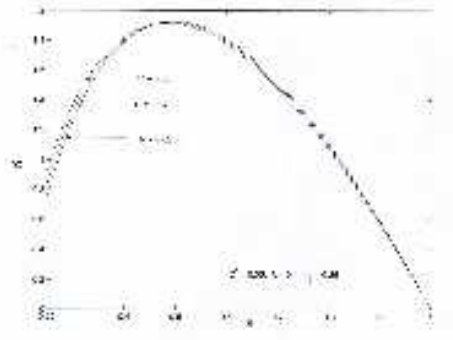

Figure 4: Variation of Axial Velocity (for fixed C^*)

4.2 Pressure drop

The non-dimensional pressure drop, p^*, across the annulus is obtained from the equations (9), (10) and (12) following [7]. It is defined as

$$p^* = \frac{2f'}{R} - \frac{f^2}{2\eta} \tag{41}$$

As an illustration, we have shown the variation of p^* for $C^* = 0.05, \lambda = 0.1, \eta_0 = 0.25$ and $R = 0.02$ in the 6. The pressure profile assumes maximum in the central region.

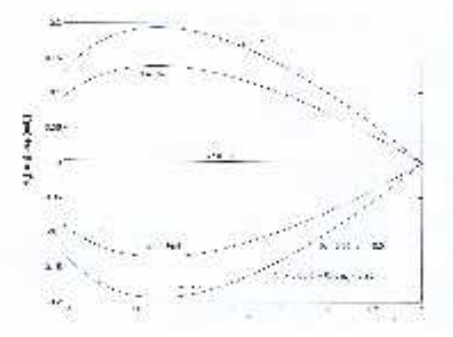

Figure 5: Variation of Unsteady Axial Velocity

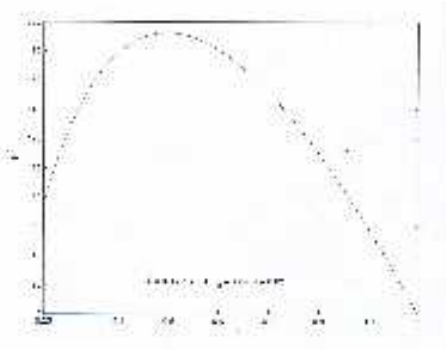

Figure 6: Variation of Pressure Drop (for fixed C^* and R)

4.3 Skin friction

The shear stress on the surface of inner cylinder is given by

$$(\tau_{rz})_{wall} = \mu \left(\frac{\partial w}{\partial r} + \frac{\partial u}{\partial z} \right)$$

Using (7), (8), (11) and (12) we get

$$(\tau_{rz})_{wall} = \frac{2\mu V \eta_0^{1/2}}{b} \left[-2z^* f''(\eta_0) + g'(\eta_0) + \mathrm{Re}\left\{ L^* h'(\eta_0) \exp(i\omega t) \right\} \right] \quad (42)$$

where $z^* = \dfrac{z}{b}$ and $L^* = \dfrac{L_4 b^2}{4\nu V}$

We define a coefficient of skin-friction in the non-dimensional form as

$$C_F = \frac{b}{2V\mu} (\tau_{rz})_{wall} \quad (43)$$

Using (18), (19) and (42) in equation (43) we have

$$C_F = \frac{\eta_0^{1/2}}{\lambda} \left[\left(2z^* - \frac{d}{\beta} \right) (\beta C^* - f') + L^* \,\mathrm{Re}\left\{ (h - C^*) \exp(i\omega t) \right\} \right] \quad (44)$$

The variation of $C_F^* \left(\equiv \lambda C_F / \eta_0^{1/2} \right)$ has been shown against ωt in Fig. 7. It is noted that the variation in the values of $|C_F^*|$ increases with increase in L^* during one period. Even though the periodic character of the profile is maintained, the amplitude is relatively less in case of $L^* = 0.5$.

5 Numerical solution and comparison

The perturbation results of section 3 are strictly valid only when $\in = 0(1)$ and $\alpha^2 = 0(1)$. To test the accuracy of these results we need to integrate

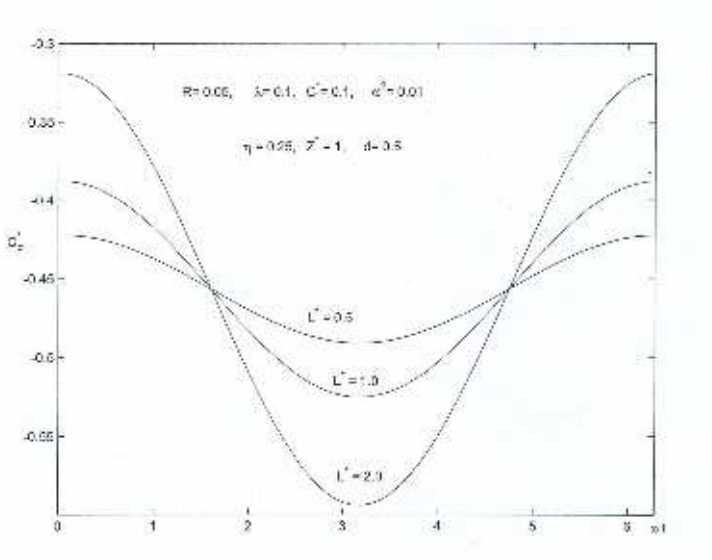

Figure 7: Variation of Skin-friction

the governing equations numerically. To solve the two-point boundary value problem expressed by equations (22), (23) and (17) - (**??**), we apply a shooting and matching technique. The resulting equations were integrated by the use of the Numerical Algorithms Group (NAG) subroutine (D02 AGF) which solves the two-point boundary value problem for a system of ordinary differential equations, using the initial value techniques (D02 ABF) and Newton iteration. The D02 AGF subroutine requires initial estimates for the unknown boundary conditions at $\eta = \eta_0$ and $\eta = 1$. For $\in = 0\,(1)$ and $\alpha^2 = 0\,(1)$, these missing values were provided by the regular perturbation results of section 3. This being successful, results for larger values of $\in$ and α^2 can be obtained by progressively increasing $\in$ and α^2 by small amounts and estimating the unknown boundary conditions from the previously computed set of results, as in Hamza [17].

	$\|f(\eta)\|$		$\|h(\eta)\|$	
η	Perturbation	Numerical	Perturbation	Numerical
0.40	0.2073	0.2003	0.1902	0.1902
0.55	0.4913	0.4846	01829	0.1829
0.70	0.7520	0.7481	0.1408	0.1408
0.85	0.9335	0.9323	0.0775	0.0775

Table 1: Comparison of Perturbation and Numerical Solutions for $R = 0.02$, $C^* = 0.05$, $\lambda = 0.10$, $\alpha = 0.10$

The comparison of $|f(\eta)|$ and $|h(\eta)|$ obtained by perturbation and numer-

ical solution for small suction case has been presented in the Table 1. The tabulated values show a good agreement of the results up to four decimal places.

6 Appendix: Derivation of equations (18) - (19)

Equation (7) shows $\dfrac{\partial u}{\partial z} = 0$ From (8) and (11) we have

$$w = -\frac{1}{r} z F'(r) + G(r) + \operatorname{Re}\left[H(r) \exp(i\omega t)\right],$$
$$\frac{\partial w}{\partial r} = \frac{1}{r^2} z F'(r) - \frac{1}{r} z F''(r) + G'(r) + \operatorname{Re}\left[H'(r) \exp(i\omega t)\right] \qquad (45)$$

Assuming continuity of pressure at the interface of free fluid region and permeable medium, (4), (9) and (10) give

$$W = \frac{k\rho}{\mu}\left[2L_1 Z - L_2 + \operatorname{Re}\left\{L_4 \exp(i\omega t)\right\}\right] \qquad (46)$$

Using equations $\dfrac{\partial u}{\partial z} = 0$, (45) and (46) in (6) at the inner cylinder $r = a$, we have

$$\frac{z}{a}\left[F'(a)\left(\frac{1}{a} + \gamma\right) - F''(a)\right] + G'(a) - \gamma G(a) +$$
$$\operatorname{Re}\left[\left\{H'(a) - \gamma H(a)\right\} \exp(i\omega t)\right] + \frac{\gamma k\rho}{\mu}\left[2L_1 z - L_2 + \operatorname{Re}\left\{L_4 \exp(i\omega t)\right\}\right] = 0$$

Equating the coefficients of z, terms independent of z and coefficients of $\exp(i\omega t)$, we have

$$\frac{1}{a} F'(a)\left(\frac{1}{a} + \gamma\right) - \frac{1}{a} F''(a) + \frac{2L_1 \gamma k\rho}{\mu} = 0$$

$$G'(a) - \gamma G(a) - \frac{\gamma k\rho L_2}{\mu} = 0, \quad H'(a) - \gamma H(a) + \frac{\gamma k\rho L_4}{\mu} = 0. \qquad (47)$$

On using the continuity requirement of radial velocity at $r = a$, equation (7) gives$F(a) = 0$ Introducing non-dimensional variables and parameters defined by (12), (16) and (20) in (47) and $F(a) = 0$, we get equations (18) through (**??**). Using (7) and (8) in the boundary conditions at the outer cylinder (5) and following similar procedure we get (17).

Acknowledgements: Thanks are due to the referee for his comments, which led to the improvement of the paper. One of the authors (SCR) gratefully acknowledges the facilities extended when he was visiting Department of Mathematics and Statistics, Sultan Qaboos University, Muscat, Oman.

References

[1] R. M. Terrill: Flow through a porous annulus, Appl. Sci. Res. 17 (1967) 204.

[2] R. M. Terrill: Fully developed flow in a permeable annulus, J. Appl. Mech. 35 E (1968) 184.

[3] C. L. Huang: Applying quasilinearization to the problem of flow through an annulus with porous walls of different permeability, Appl. Sci. Res. 29 (1974) 145.

[4] P. D. Verma and Y. N. Gaur: Laminar swirling flow in an annulus with porous walls, Proc. Indian Acad. Sci. 80 A (1974) 211.

[5] F. M. Skalak and C. Y. Wang: Pulsatile flow in a tube with wall injection, Appl. Sci. Res. 33 (1977) 269.

[6] P. D. Verma and Y. N. Gaur: Unsteady flows of an incompressible viscous fluid in a porous annulus, Indian J. Phys. 46 (1972) 203.

[7] Mohan Singh and S. C. Rajvanshi: Pulsatile flow in a porous annulus for small Reynolds number, J. Math. Phys. Sci. 20 (1986) 391.

[8] Mohan Singh and S. C. Rajvanshi: Pulsatile flow in a porous annulus for large suction, Proc. Indian natn. Sci. Acad. 53 A (1987) 622.

[9] R. C. Choudhary and T. Chand: Three dimensional flow and heat transfer through a porous medium, Int. J. Appl. Mech. & Engg. 7 (2002) 1141

[10] G. S. Beavers and D. D. Joseph: Boundary conditions at a naturally permeable wall, J. Fluid Mech. 30 (1967) 197.

[11] E. M. Sparrow, G. S. Beavers and L. Y. Hung: Flow about a porous-surfaced rotating disk, Int. J. Heat Mass Transf. 14 (1971) 993.

[12] P. D. Verma and B. S. Bhatt: On the steady flow between rotating and a stationary naturally permeable disc, Int. J. Engg. Sci. 13 (1975) 869.

[13] K. S. Sai: On the unsteady flow of incompressible fluid over a naturally permeable bed, J. Math. Phys. Sci. 14 (1980) 599.

[14] N. C. Sacheti: Application of Brinkman model in viscous incompressible flow through a porous channel, J. Math. Phys. Sci. 17 (1983) 567.

[15] I. P. Jones: Low Reynolds number flow past a porous spherical shell, Proc. Comb. Phil. Soc. 73 (1973) 231.

[16] Mohan Singh and S. C. Rajvanshi: Flow between rotating disks one being naturally permeable, Def. Sci. J. 39 (1989) 233.

[17] E. A. Hamza: The magnetohydrodynamic effects on a fluid film squeezed between two rotating surfaces, J. Phys. D. Appl. Phys. 24 (1991) 547.

Dirección de los autores: Elsadig A. Hamza, Dept. of Math. and Statistics College of Science, Sultan Qaboos University, Sultanate of Oman — Satish C. Rajvanshi, School of Engineering Mathematics, Institute of Engineering and Technology, Bhaddal, Mianpur Post - 140108, Ropar, India, satish_rajvanshiyahoo.co.in — Nirmal C. Sacheti, Dept. of Math. and Statistics, College of Science, Sultan Qaboos University, PO Box 36, Al Khod 123, Muscat Sultanate of Oman, nirmal@squ.edu.com.